Automatic 2D Segmentation of an Intracardiac Catheter Based on MSER Blob Detector and Eccentricity

Viacheslav V. Danilov[1], Igor P. Skirnevskiy[1], Olga M. Gerget[1], Roman A. Manakov[1]

[1] *Medical Devices Design Laboratory, RASA Center in Tomsk, Tomsk Polytechnic University, 2 Lenin Avenue, building 33, 634050 Tomsk, Russia*
E-mail: viacheslav.v.danilov@gmail.com

Abstract

The present study describes an algorithm for automatic catheter detection and segmentation based on echocardiography data. The catheter area was recognized and then delineated by combination of detection and segmentation techniques such as the maximally stable extremal regions (MSER) algorithm, feature analysis and Kittler-Illingworth thresholding algorithm. Regions processed by MSER detector were restricted by eccentricity. Eccentricity, assessing the shape of the particular region, was chosen as the main feature. Morphological closing was applied at the pre-processing step. After applying MSER blob detector, detection accuracy of the catheter made up 86.7±11.5%. After performing an additional restriction based on the shape analysis, the accuracy increased to 92.8±6.6%. The proposed algorithm allows performing automatic detection and segmentation of the catheter inside the heart based on 2D echocardiography data.

Keywords: Cardiac ultrasound, endovascular surgery, MSER, shape analysis, catheter detection.

1. Introduction

Over 25 million people worldwide suffer from cardiovascular disease (CVD) (*1*, *2*). Minimally invasive image-guided procedures such as tissue ablation or vessel stenting are used in the treatment of the CVDs (*3*). During the procedure, surgeon visualizes the target area of the intervention and the instruments indirectly using various imaging modalities. Angiography, CT or MRI are used to visualize the catheter during different minimally invasive procedures inside the heart or great vessels (*4*, *5*). Echocardiography is commonly used for perioperative diagnostics and instrument guidance, given non-invasiveness, the absence of ionizing radiation and low cost of this modality. An analysis of echocardiography is performed in a wide range of publications, studying the heart conditions or interventions visualization (*6*–*10*). Despite the advantages of echocardiography, it has a number of drawbacks such as high level of noise, the presence of image artifacts, the complexity of data interpretation and low spatial resolution. To alleviate the shortcomings described above, we proposed to use the software workflow of echocardiography image processing. This approach involved periprocedural segmentation of the intervention area and detection of the instrument (Fig. 1).

This study presents the catheter detection and segmentation algorithm based on the MSER detector and cutting off excess regions by shape analysis.

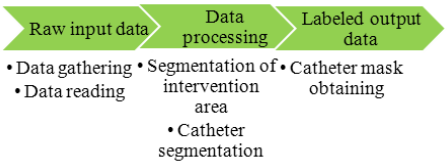

Fig. 1. The main concept of the catheter region processing and segmentation.

2. Methods and Materials

2.1. Input data

Epicardial echocardiography of porcine hearts (Yorkshire swine; weight 65–75 kg) was obtained during various image-guided beating-heart procedures. iE33 Ultrasound Machine and X7-2t transducer (Philips Healthcare, Andover MA) were used to get 9 datasets. Each dataset contained 15-17 frames, and each frame

included 208 slices with dimensions of 176*176 pixels. We attained the data at Boston Children's Hospital; the animal protocol was approved by IACUC (Institutional Animal Care and Use Committee). All animals were taken care of according to the Principles for the Care and Use of Laboratory Animals (*11*).

The desktop computer with Intel Core i7-4790K 4.0 GHz CPU, NVIDIA GeForce 960 GT GPU, 16 GB RAM was used to process the data. The algorithms were tested and implemented using MATLAB 2017a.

The Kolmogorov-Smirnov method (the distribution normality test) and the Mann-Whitney U test were used for statistical analysis.

2.2. Workflow

The main steps of the algorithm are shown in Fig. 2.

The first step of the proposed algorithm involved obtaining the data. Next, Kittler-Illingworth thresholding algorithm was applied (*12*). Then, we used morphological dilation and erosion for contours alignment, and morphological closing for fill in small background holes in images. The last and the main step of the algorithm involved applying of MSER blob detector and cutting off excess regions by eccentricity value.

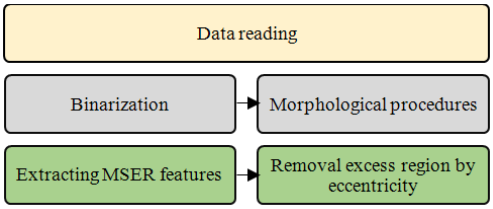

Fig. 2. Main steps of the algorithm.

2.3. Pre-processing

The first step included analysis and reduction of the digital noise. The input point of the algorithm was the binarization of the image by the Kittler-Illingworth thresholding method (*13*). That was an auto-thresholding algorithm based on minimum error. The results of the method application are shown in (b) Fig. 3a. Tissue dropouts, heterogeneity of the regions and strong distortions at the boundaries were noticeable after binarization. To solve the problem, morphological methods were used in the following sequence: erosion, dilatation, and morphological closing. Regions after performing morphological operations are shown in Fig. 3b.

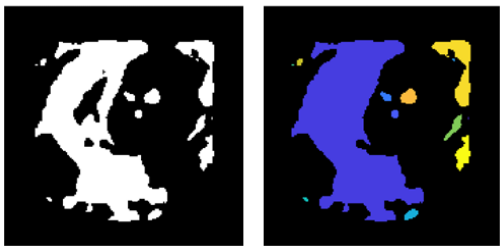

(a) (b)

Fig. 3. Image thresholding (a) and an image after applying morphological operations (b)

After performing all calculations, each region was assigned a sequence number. Additionally, several features were selected for using during next steps of the algorithm. Although, such parameters as MSE, STD and area were obtained for each region, in the present study only one metric (eccentricity) was used for identifying the region of interest.

2.4. Eccentricity

Originally, the metric was used for estimation of a planet trajectory. Astronomical object eccentricity represents a parameter, showing how much its orbit around another body differs from a perfect circle. This parameter, characterizing the ellipse elongation, is estimated as follows:

$$e = \sqrt{1 - \frac{b^2}{a^2}} \quad (1)$$

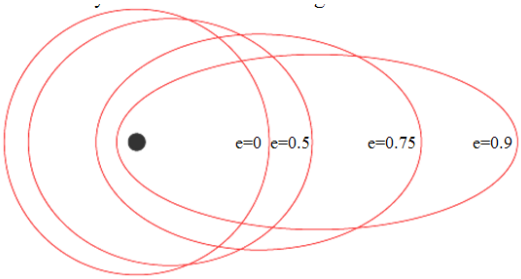

Fig. 4. Different elliptical shapes depending on the eccentricity value.

where a and b – the lengths of semi-major and semi-minor axis respectively. As it can be seen, eccentricity varies for elliptical shapes in (0, 1) range and it is equal to 0 for a perfect circle. Different values of the eccentricity are shown below in Fig. 4.

Eccentricity was chosen for the current study because of the high similarity of the binarized catheter region with ellipse and/or circle. Such similarity was observed within all datasets. Two examples of elliptical and circular shapes of the catheter are shown in Fig. 5.

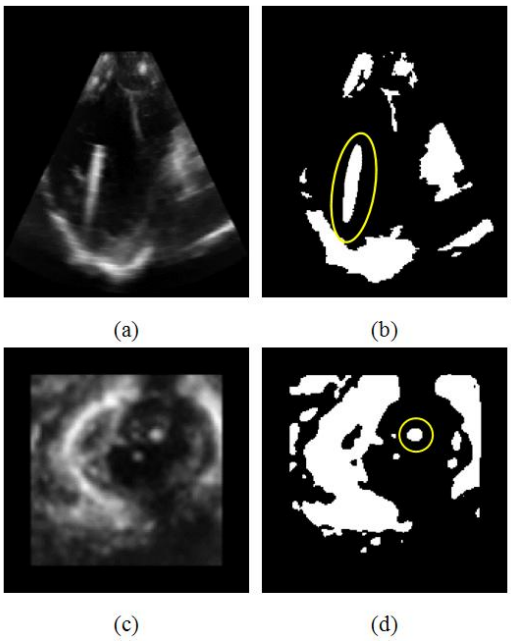

Fig. 5. Slice of long-axis view (a) and its automatic thresholding (b), slice of short-axis view (c) and its binarization (d).

2.5. MSER detector

We used the Maximally Stable Extremal Regions method for initial regions extraction. The MSER is a feature detector used as a method of blob detection (*14*). The MSER method involved extraction of co-variant or "stable" regions from an image. The main advantages of MSER algorithm include:

(i) Invariance to an affine transformation of intensities (*15*).
(ii) Covariance to adjacency continuous transformation (*14*, *16*).
(iii) Multi-scale detection. Detection of MSERs in a scale pyramid improves repeatability and number of correspondences across scale changes (*17*).
(iv) The set of all extremal regions can be enumerated in worst-case $O(n)$, where n is the number of pixels in the image (*16*).

Use of other detectors such as SIFT (Scale-Invariant Feature Transform) has been described (*18–20*). However, in the present study, use of the MSER detector was appropriate. The latter was confirmed empirically. During the experiments, we used the following parameter values for the proposed algorithm: max area variation ranged from 0.15 to 0.25, threshold delta ranged from 1% to 4%.

2.6. Removal of false MSER regions

To detect the region of the catheter properly, all regions obtained after MSER blob detector application were sorted by the eccentricity with the minimum and maximum boundary conditions shown in Fig. 6.

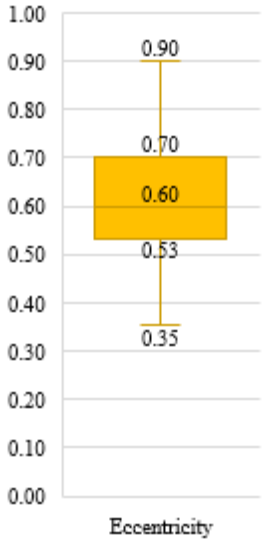

Fig. 6. Distribution of the eccentricity within the frame.

Based on 208 slices of echocardiography short axis view, the average value of the catheter eccentricity was 0.62, which proved that the catheter image was displayed as an elliptical shape. However, the metric ranged from 0.35 (minimum boundary) to 0.90 (maximum boundary).

3. Results

3.1. Data processing

After the initial steps were applied (see Fig. 3), each image was divided into the regions, and each region had certain properties. Depending on echocardiography image slice, we obtained on the average from 9 to 14 regions. Fig 7 represents an example with 13 regions where the catheter is shown as the region №7.

Fig. 7. Regions of the slice.

After applying the MSER detector with a simple area correction, we obtained a list of regions that could potentially be the catheter region. Fig. 8 shows the results of the MSER algorithm. The use of the MSER detector reduced the number of regions from 13 to 3 on the example slice. A similar reduction in the number of potentially catheter regions was observed in all slices during the experiment. On the average, the number of regions after applying the MSER algorithm with area limitations was reduced by 70%.

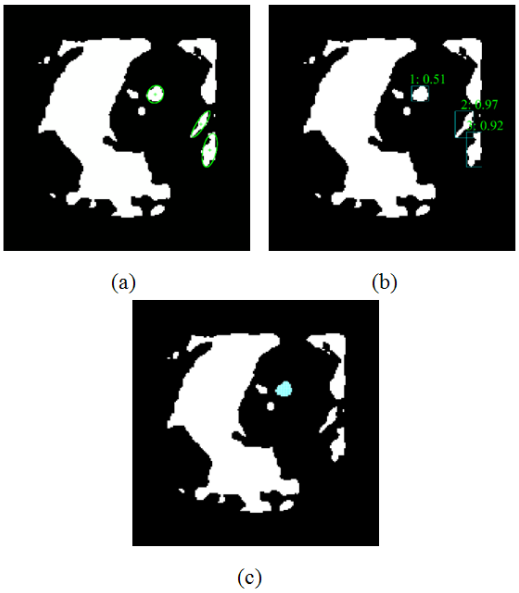

Fig. 8. Drawing of elliptical frames (a), eccentricity estimation (b), pixel list/segmentation of the catheter region (c).

The final step involved the estimation of the regions eccentricity. The eccentricity on all processed slices as mentioned above varied from 0.35 to 0.90. Green ellipses have a second moment equivalent to the region-of-interest in Fig. 8a. Fig. 8b shows an estimation of the eccentricity values of the studied areas. In Fig. 8b, eccentricity values of regions №2 and №3 do not fall under the condition of the eccentricity criterion, thus these regions are false. After sorting the remaining regions by eccentricity value, the region was drawn and replaced by an ellipse that had a second moment equivalent to the studied region. This solution was used to draw the real projection of the ellipse because the region of the catheter was not always displayed properly after the binarization. The final results of the algorithm are shown in Table 1.

Measured diameter of the processed catheter region deviated from the reference value by 5.5%. The absolute average error of 0.129 mm does not strongly influence on the visualization of the anatomical structures of the heart and medical instruments. Combination of the MSER blob detector and eccentricity improved efficiency of the algorithm. The efficiency of the MSER application without and with eccentricity restriction were 86.7±11.5% and 92.8±6.6% respectively. Consequently, eccentricity allowed localizing the catheter with a high level of accuracy. Only 6.8% of false regions remained after sorting by eccentricity.

According to the Kolmogorov-Smirnov criterion, the sample consisting of 52 elements (measured diameters) turned out to be not normal. The result of the non-parametric test (Mann-Whitney test) at 1% significance level was as follows: h = 0 and p = 0.0113, which indicated that there were no differences between the samples.

3.2. Processing time

The processing time of the algorithm was estimated on the computer (see «Input data» section). The measuring process was not isolated from other processes. For the processing time assessment, 200 iterations were performed. The average execution time for processing of 176*176 slice was 8±0.57 ms.

4. Conclusion

We developed the algorithm that allowed performing fully automatic two-dimensional catheter detection and segmentation based on echocardiography data. The proposed algorithm was based on the method of determining the extreme stable regions (MSER blob detector). The final step of the algorithm included shape analysis and removed excess regions by eccentricity limitations. When working with objects of elliptical shape, the use of this feature was very effective. Out of 12 regions received by the means of the MSER detector, no more than 16% of the sample remained after eccentricity restriction. In the present study eccentricity value was established empirically. It can vary depending on the type and shape of the medical device, position of the echocardiography transducer.

Acknowledgments

This study was supported by the Russian Federation Governmental Program ‘Nauka’ № 12.8205.2017/БЧ (addition number: 4.1769.ГЗБ.2017) and the Tomsk Polytechnic University Competitiveness Enhancement Programme grant.

Table 1. Results of the proposed algorithm.

	Assessment of the catheter diameter	
	Real value	Measured value
Mean, mm	2.333	2.462
STD, mm	0.00	0.31
Error, %	0.00	5.56

	Estimation of the catheter region detection error			
	Error		Efficiency	
	MSER	MSER + eccentricity	MSER	MSER + eccentricity
Mean±STD, %	13.3±11.5	6.8±6.6	86.7±11.5	92.8±6.6

References

1. P. Ponikowski *et al.*, Heart failure: preventing disease and death worldwide. *ESC Hear. Fail.* **1**, (2014) 4–25
2. WHO | Cardiovascular diseases (CVDs). *WHO* (2016).
3. D. M. Kwartowitz, F. N. Mefleh, G. H. Baker, Toward computer-assisted image-guided congenital heart defect repair: an initial phantom analysis. *Int. J. Comput. Assist. Radiol. Surg.* **12**, (2017) 1839–1844.
4. A. Baszko *et al.*, www.kardiologiapolska.pl Value of rotational angiography (3D−ATG) with contrast agent administration into the right atrium during atrial fibrillation ablation procedures: a preliminary report. *Kardiol. Pol.* **70**, (2012) 924–930.
5. A. Hernandez-Vela *et al.*, Accurate Coronary Centerline Extraction, Caliber Estimation, and Catheter Detection in Angiographies. *IEEE Trans. Inf. Technol. Biomed.* **16**, (2012) 1332–1340.
6. V. V Danilov, I. P. Skirnevskiy, O. M. Gerget, Segmentation of anatomical structures of the heart based on echocardiography. *J. Phys. Conf. Ser.* **803**, 1–6 (2017).
7. V. V. Danilov *et al.*, Efficient workflow for automatic segmentation of the right heart based on 2D echocardiography. *Int. J. Cardiovasc. Imaging*. **34**, (2018) 1–15.
8. K. Fattouch *et al.*, Papillary muscle relocation and mitral annuloplasty in ischemic mitral valve regurgitation: Midterm results. *J. Thorac. Cardiovasc. Surg.* **148**, (2014) 1947–1950.
9. J. S. Yoo *et al.*, Mitral durability after robotic mitral valve repair: Analysis of 200 consecutive mitral regurgitation repairs. *J. Thorac. Cardiovasc. Surg.* **148**, (2014) 2773–2779.
10. L. Yan *et al.*, Ultrasound-Guided Intratumoral Radiofrequency Ablation Coagulation to Facilitate Meningioma Resection: Preliminary Experience. *J. Ultrasound Med.* (2017), doi:10.1002/jum.14365.
11. J. D. Clark, G. F. Gebhart, J. C. Gonder, M. E. Keeling, D. F. Kohn, The 1996 Guide for the Care and Use of Laboratory Animals. *ILAR J.* **38**, (1997) 41–48.
12. J. Kittler, J. Illingworth, J. Föglein, Threshold selection based on a simple image statistic. *Comput. Vision, Graph. Image Process.* **30**, (1985) 125–147.
13. J. Kittler, J. Illingworth, Minimum error thresholding. *Pattern Recognit.* **19**, (1986) 41–47.
14. J. Matas, O. Chum, M. Urban, T. Pajdla, in *Image and Vision Computing* (2004), vol. 22, pp. 761–767.
15. K. Mikolajczyk *et al.*, A Comparison of Affine Region Detectors. *Int. J. Comput. Vis.* **65**, (2005) 43–72.
16. D. Nistér, H. Stewénius, in *Lecture Notes in Computer Science (including subseries Lecture Notes in Artificial Intelligence and Lecture Notes in Bioinformatics)* (2008), vol. 5303 LNCS, pp. 183–196.
17. P. E. Forssén, D. G. Lowe, in *Proceedings of the IEEE International Conference on Computer Vision* (2007).
18. G. Wang, J. Wang, SIFT Based Vein Recognition Models: Analysis and Improvement. *Comput. Math. Methods Med.* **2017**, (2017) 1–14.
19. Y. He *et al.*, in *Advances in experimental medicine and biology* (2017) vol. 977, pp. 183–190.; http://www.ncbi.nlm.nih.gov/pubmed/28685444),
20. S. L. Al-khafaji, J. Zhou, A. Zia, A. W.-C. Liew, Spectral-Spatial Scale Invariant Feature Transform for Hyperspectral Images. *IEEE Trans. Image Process*, 1–1 (2017).